PHYSICAL REVIEW B **81**, 220404(R) (2010)

# Growth and magnetic order of Mn films on Fe(001)-$p(1\times1)$O studied by spin-polarized scanning tunneling microscopy

Achiri Tange,[1] Chunlei Gao,[1] Wulf Wulfhekel,[1,2] and Jürgen Kirschner[1]
[1]*Max-Planck-Institut für Mikrostrukturphysik, Weinberg 2, D-06120 Halle, Germany*
[2]*Physikalisches Institut, Karlsruher Institut für Technologie (KIT), 76131 Karlsruhe, Germany*
(Received 17 January 2010; revised manuscript received 3 May 2010; published 3 June 2010)

Mn films show improved layer-by-layer growth on the Fe(001)-$p(1\times1)$O surface compared to the clean Fe(001) surface. From Auger electron spectroscopy the surfactant role of the oxygen was confirmed. A layerwise antiferromagnetic order in the Mn films is preserved as seen from the magnetic contrast between adjacent Mn layers in spin-polarized scanning tunneling microscopy while the surface spin polarization is enhanced by a factor 2 compared to Mn films grown on the clean Fe(001) surface. Further, topologically induced magnetic frustrations of the Mn layer above buried Fe steps appear wider than without oxygen.

DOI: 10.1103/PhysRevB.81.220404 PACS number(s): 75.70.Rf, 68.37.Ef, 75.50.Ee

The interaction between a ferromagnet and an antiferromagnet forms the basis of exchange bias but is currently not well understood as the mechanisms occurring at the interface are not completely known. Antiferromagnetic thin films are widely used in modern magnetic storage devices and will play a major role in future storage devices such as magnetic random-access memories. Understanding the structural as well as magnetic properties of these structures is of utmost importance in understanding the properties of devices.

Bulk manganese has a complex structure and exhibits different phases which show different magnetic behavior depending on the ambient conditions.[1] The stable bulk phase at temperatures up to 1000 K is the complex cubic $\alpha$-Mn which has 58 atoms per unit cell[2] and shows antiferromagnetism below 95 K.[3] At higher temperatures three different cubic phases exist.[4] Due to these high temperatures these structures are difficult to characterize.

By choosing an appropriate substrate, similar phases of Mn can be stabilized at room temperature by epitaxy. On Fe(001), Mn stabilizes in a body-centered tetragonal (bct) structure adopting the in-plane lattice constant of the Fe(001) substrate ($a=b=2.866$ Å) and an out-of-plane lattice constant of $c=3.228$ Å.[5] The bct structure persists up to thicknesses between 10 monolayers (ML) to 25 ML depending on the deposition conditions.[6–8] Above this thickness there is a transition to $\alpha$-Mn displaying a complex and noncollinear spin structure.[9] Bct manganese films on bare Fe(001) show a layerwise antiferromagnetic order.[10–12]

Because the magnetoresistance properties of tunnel junctions depend strongly on the spin polarization at the interfaces between the ferromagnetic metal and the insulating layer it is important to understand how the magnetic properties of metallic surfaces change with the presence of oxygen. This is in analogy to oxygen diffusion into the metals from the insulating layer. Here we investigate the effect an ordered oxygen monolayer on Fe(001) has on the growth and magnetic order of thin Mn films. We show that by growing Mn films on Fe(001)-$p(1\times1)$O, one can extend the layer-by-layer growth regime, with the O playing a surfactant role. The surface is more stable to contaminations and the spin contrast observed between adjacent Mn layers is enhanced compared to Mn films grown on the bare Fe(001) surface.[13] In addition, magnetic frustrated regions, that occur where the Mn film overgrows an Fe substrate step, appear much wider.

The experiments were carried out in an ultrahigh-vacuum chamber (base pressure less than $2\times10^{-10}$ mbar) equipped with an Auger electron spectrometer (AES), a low-energy electron-diffraction (LEED) system and a room-temperature spin-polarized scanning tunneling microscope (Sp-STM). The iron whiskers substrates were cleaned by $Ar^+$ bombardment and annealing. The cleanliness was checked with AES and LEED. The Fe(001)-$p(1\times1)$O surface was prepared by exposing the clean Fe(001) surface to 6 L of oxygen ($1\ \mathrm{L}=1.33\times10^{-6}$ mbar s) and subsequent annealing to 700 K.[14] The Sp-STM used in our experiments operates in the differential magnetic mode.[15,16] By using a soft ferromagnetic material in the form of a ring for the STM electrode, the in-plane component of the sample spin polarization can be measured (due to shape anisotropy the magnetization of the ring lies tangential to its outer perimeter).[12] With a coil wound around the ring, its magnetization is switched periodically between two stable states by applying a high-frequency alternating current through the coil. The resulting change in the tunneling current due to the magnetization reversal of the ring is detected with a phase-sensitive lock-in amplifier. This change, which is proportional to the projection of the sample spin polarization onto the ring plane, is purely of magnetic origin. It is separated from the average tunneling current, which serves as the input for the STM feedback loop yielding the surface topography. Thus spin signal and topography can be detected separately but are acquired simultaneously in a single experiment. The Mn films were deposited by electron-beam evaporation from Mn flakes held in a Mo crucible. The substrate was kept at about 400 K during deposition while the pressure in the chamber stayed well below $5\times10^{-10}$ mbar. In the preparation chamber, the AES gun is located opposite the LEED screen such that the combination of the AES gun and the LEED optics can be used as a medium-energy electron-diffraction (MEED) system to monitor film thickness during deposition. The deposition was carried out at a rate of approximately 0.5 ML/min as determined from the periodicity of the MEED oscillations.

Figure 1(a) shows the MEED intensity during growth of

 

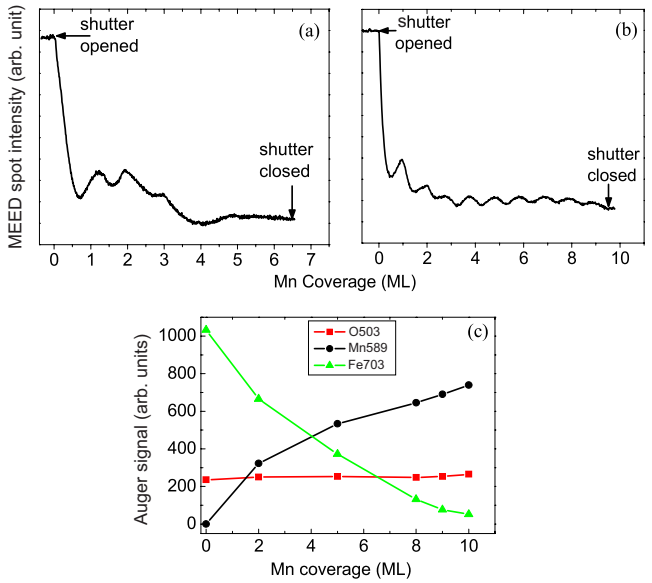


FIG. 1. (Color online) MEED intensity oscillations for Mn deposited onto (a) bare Fe(001) and onto (b) Fe(001)-$p(1\times1)$O. (c) Peak intensities for the principal Auger peaks for O (503 eV), Mn (589 eV), and Fe (703 eV) as a function of Mn film thickness for Mn deposited onto Fe(001)-$p(1\times1)$O.

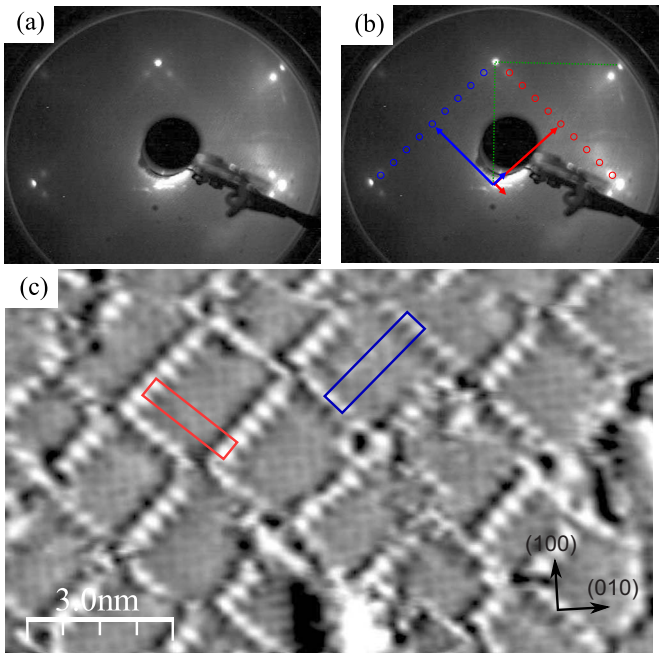


FIG. 2. (Color online) (a) 55 eV LEED pattern of 9.4 ML Mn deposited onto Mn/Fe(001)-$p(1\times1)$O. (b) A two domain superstructure explains the observed pattern. Green dotted lines indicate the primitive reciprocal-lattice vectors of the Fe(001) and red (light gray) and blue (dark gray) arrows the supercell reciprocal-lattice vectors. Expected LEED spots of the two domains are indicated with open circles. (c) Atomically resolved STM image of the same film indicating the same two domain superstructure as indicated by boxes ($I$=3.1 nA and $U$=20 mV).

6.5 ML Mn on Fe(001). During the growth, it displays an initial drop followed by three maxima and a constant intensity. The oscillations in the MEED intensity indicate a layer-by-layer growth mode only for the first 3 ML. Reflection high-energy electron-diffraction and x-ray absorption fine structure measurements[5,7] have shown that the interlayer spacing of Mn films up to 2 ML are slightly smaller than for thicker films, hinting at a change the crystallographic details at 3 ML coverage. This modification of the lattice constant could be responsible for this change of the growth mode. The disappearance of the MEED oscillations could result from an increase in the adatom mobility and thus from a transition to step-flow growth. In step-flow growth, the roughness of the surface does not change with coverage and the MEED intensity is stable, in agreement with the relatively flat topography of thicker films observed with STM.[13] Figure 1(b) shows the MEED intensity oscillations during growth of 9.5 ML Mn on Fe(001)-$p(1\times1)$O. One observes more oscillations in the MEED intensity compared to the case on the bare Fe(001) surface and no transition to step-flow growth. Figure 1(c) depicts the peak intensities for the principal Auger peaks for O (503 eV), Mn (589 eV), and Fe (703 eV) as a function of Mn film thickness for Mn/Fe(001)-$p(1\times1)$O. While the Mn signal increases with thickness, the Fe signal decreases almost to zero, showing that there is little or no alloying or Fe segregation in thick films. The O intensity does not show any significant change with film thickness. This indicates that the oxygen atoms float on top of the surface acting as a surfactant to promote layer-by-layer growth.

Interestingly, the LEED pattern changes from a $(1\times1)$ structure of the Fe(001)-$p(1\times1)$O surface to a more complex structure after Mn growth as indicated in Fig. 2(a). Near to the principal spots, four additional spots are visible as well as a faint lines between first-order spots. This can be explained by the formation of a reconstruction at the surface involving the floating oxygen. The reconstruction is of a two domain $(\sqrt{50}\times\sqrt{2})R45°$ type. Figure 2(b) shows in green dotted lines the reciprocal-lattice vectors of the Fe(100) surface and the reciprocal-lattice vectors of the two domains of the reconstruction in red and blue arrows. The expected diffraction peaks are marked with circles. The LEED pattern clearly shows the first-order spots of the superstructure. At the position of the higher-order spot, an enhanced intensity in form of lines can be seen. This indicated that there is mainly local order and only weak long-range order beyond the unit cell of the reconstruction. The reconstruction was visible for thinner films (<4 ML) as well. From our LEED and MEED data, one can speculate that the lack of change in the growth mode is related to the presence of the reconstruction. Alternatively, it could be due to a suppression of the slight structural transformation at 3 ML coverage in the presence of oxygen. The latter could, however, not be verified by LEED-IV measurements, as the diffraction pattern is rather blurred prohibiting a quantitative LEED-IV analysis.

In agreement with the above analysis of the LEED pattern, atomically resolved STM images [see Fig. 2(c)] display lines running along [110] directions, i.e., along 45° with respect to the [100] directions. The unit cell of the $(\sqrt{50}\times\sqrt{2})R45°$ is indicated in the figure. While the lines are rather straight, long-range order is far from perfect, explaining the lack of higher-order diffraction peaks in LEED. As AES indicated a floating of oxygen, the reconstruction is

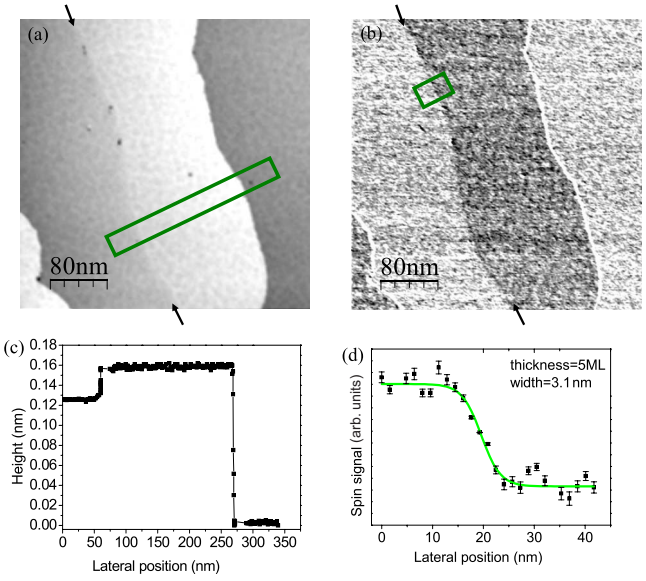


FIG. 3. (Color online) (a) Topography and (b) corresponding spin signal for 5 ML Mn grown on oxygen covered Fe(001) ($I$=3.7 nA and $U$=220 mV). The arrows indicate the position of a buried Fe step. (c) Averaged line scan taken within the green rectangle in (a). (d) Line scan taken along the green rectangle in (b). The error bars are the standard deviation from the mean of ten different line scans.

most probable caused by the formation of a surface layer of MnO that forms a large supercell due to its lattice mismatch with the substrate lattice. To relax some of the strain, antiphase boundaries in form of the white lines in the STM images are formed. As these antiphase boundaries induce nearest-neighbor hollow sites to be occupied by oxygen atoms, it is energetically not favorable for different antiphase boundaries to meet in one point. Thus the antiphase boundaries of adjacent domains are shifted by one atomic distance as observed in the STM image.

The topography of 5 ML Mn/Fe(001)-$p(1\times1)$O is shown in Fig. 3(a). The surface has Mn terraces about 200 nm wide separated by monatomic steps, as indicated in the line scan [see Fig. 3(c)] taken along the green rectangle. The terraces display a slight corrugation due to the oxygen-induced reconstruction. Also visible is a step of subatomic height caused by the vertical lattice mismatch between Mn and Fe as the Mn film overgrows a step of the underlying Fe substrate (indicated by the arrows). The line scan in Fig. 3(c) confirms the presence of such subatomic steps of height about 0.03 nm. The spin image corresponding to the topography is shown in Fig. 3(b). On the right side of the image, one observes a spin contrast between Mn terraces separated by a monatomic step. The orientation of the ring plane, i.e., the direction of spin sensitivity of the ring, was aligned with the long whisker axis. Due to the simple magnetic configuration of whiskers with large domains aligned along the long whisker axis, the magnetic moments of the underlying Fe whisker is parallel to the direction of sensitivity of the Sp-STM. The large contrast on the Mn film indicates a layerwise antiferromagnetic order within the Mn film with alternating projection onto the direction of sensitivity.[17] On the left of

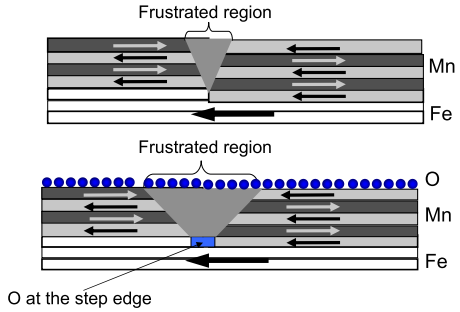


FIG. 4. (Color online) Schematic of the frustrated region. Top: Mn/Fe(001). Bottom: Mn films deposited onto Fe(001)-$p(1\times1)$O.

the image at the position of the buried Fe step (indicated by the arrows), one observes a magnetic contrast. At the position of the buried Fe step, $n$ Mn layers were grown on the upper side while $n+1$ layers were grown on the lower side of the step edge. The moments of the bottom Mn atoms on both sides of the step edge exchange couple identically to the Fe substrate[18] and are therefore aligned in the same direction in the plane with respect of the Fe substrate. Due to the atomic Fe step edge, however, an ideal layerwise antiferromagnetic order is not possible around the step edge. Instead, a magnetic frustration is observed in the Mn layers that meet at such steps. They are polarized in opposite directions,[11,19] i.e., a situation similar to a 180° domain wall is present. A schematic of such a frustration is shown in Fig. 4 for both Mn/Fe(001) and Mn/Fe(001)-$p(1\times1)$O. Figure 3(d) indicates the averaged line profile taken along the green rectangle in Fig. 3(b) across the frustrated region. To estimate the width of the frustrated region, the profile has been fitted with a hyperbolic tangent function, which represents the analytical solution for a 180° domain wall if dipolar energies are neglected.[20] The green line represents the tanh-function fit from which the width has been estimated to be $3.1\pm0.1$ nm. At a thickness of 6 ML (not shown) the width increases to $4.0\pm0.1$ nm. Note that the width of the frustrated region is independent of the step direction, as it is not induced by anisotropy but by the exchange, which is direction independent in first order.[18] For Mn films of similar thickness grown on Fe(001) the width of the frustrated region is much smaller

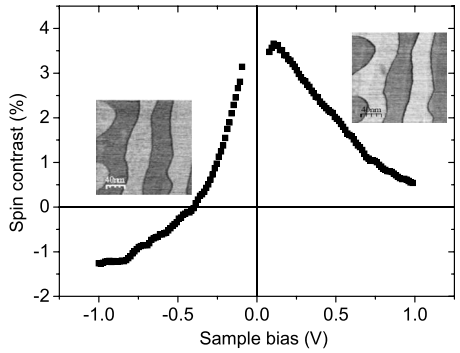


FIG. 5. Spin contrast as a function of the sample bias. The insets show the spin image at 0.5 V (right) and −0.5 V (left), respectively. A reversal of the contrast occurs at −0.4 V. Tunneling current was 1 nA.

($1.6 \pm 0.3$ nm at a thickness of 5.5 ML).[18] The wider frustrated region can be explained by some oxygen being present at the buried step edges of the substrate (see Fig. 4), locally lowering the exchange within the Mn near the step edge, within the Fe substrate or the pinning to the Fe substrate and thus cause the frustration to be less localized. The presence of some oxygen (or oxides) at the surface could further reduce the exchange. Thus, small amounts of adsorbed species around buried step edges might lead to modifications of the wall width in general. This offers a possibility to explain the different observed widths for Mn/Fe(001).[11,19,21]

The spin contrast between adjacent Mn terraces separated by a monatomic step as a function of applied voltage is shown in Fig. 5. It is defined as the difference of the lock-in signal observed on the two terraces. It shows a similar voltage dependence as for Mn films grown on the bare Fe(001) surface.[13] The maximum spin contrast occurs around 0.1 V. It is positive for all measured positive bias voltages and changes sign around −0.4 V. In the case for Mn deposition onto Fe(001)-$p(1 \times 1)$O, the spin contrast is larger by a factor 2 than on Mn films deposited onto bare Fe(001) for identical tunneling conditions. This indicates that the surface spin polarization is enhanced by the oxygen overlayer. This could result from a spin polarization of the oxygen on the surface due to interaction with Mn *d* orbitals.[22]

In conclusion, we demonstrated that oxygen can be used as a surfactant mediating layer-by-layer growth for antiferromagnetic Mn on Fe(001). Further, we demonstrated that the oxygen has effects on the magnetic properties of the Mn layer. While it does not affect the layerwise antiferromagnetic order, it increases the spin polarization of the surface. Further, it decreases the exchange coupling at buried Fe step edges leading to widening of the frustrated regions highlighting the role of adsorbates at step edges on frustrations.

[1] D. Hobbs, J. Hafner, and D. Spišák, Phys. Rev. B **68**, 014407 (2003).
[2] A. J. Bradley and J. Thewlis, Proc. R. Soc. London, Ser. A **115**, 456 (1927).
[3] R. Tebble and D. Craik, *Magnetic Materials* (Wiley-Interscience, London, 1969).
[4] R. W. Wyckoff, *Crystal Structures* (Interscience-Publication, New York, 1963).
[5] S. K. Kim, Y. Tian, M. Montesano, F. Jona, and P. M. Marcus, Phys. Rev. B **54**, 5081 (1996).
[6] S. T. Purcell, M. T. Johnson, N. W. E. McGee, R. Coehoorn, and W. Hoving, Phys. Rev. B **45**, 13064 (1992).
[7] S. Andrieu, M. Finazzi, P. Bauer, H. Fischer, P. Lefevre, A. Traverse, K. Hricovini, G. Krill, and M. Piecuch, Phys. Rev. B **57**, 1985 (1998).
[8] E. C. Passamani, B. Croonenborghs, B. Degroote, and A. Vantomme, Phys. Rev. B **67**, 174424 (2003).
[9] C. L. Gao, U. Schlickum, W. Wulfhekel, and J. Kirschner, Phys. Rev. Lett. **98**, 107203 (2007).
[10] T. G. Walker and H. Hopster, Phys. Rev. B **48**, 3563 (1993).
[11] T. K. Yamada, M. M. J. Bischoff, G. M. M. Heijnen, T. Mizoguchi, and H. van Kempen, Phys. Rev. Lett. **90**, 056803 (2003).
[12] U. Schlickum, W. Wulfhekel, and J. Kirschner, Appl. Phys. Lett. **83**, 2016 (2003).
[13] U. Schlickum, C. L. Gao, W. Wulfhekel, J. Henk, P. Bruno, and J. Kirschner, Phys. Rev. B **74**, 054409 (2006).
[14] A. Tange, C. L. Gao, A. Ernst, W. Wulfhekel, and J. Kirschner, Phys. Rev. B **81**, 195410 (2010).
[15] W. Wulfhekel and J. Kirschner, Appl. Phys. Lett. **75**, 1944 (1999).
[16] W. Wulfhekel and J. Kirschner, Annu. Rev. Mater. Res. **37**, 69 (2007).
[17] There is a weak bright contrast on the downsteps induced by crosstalk from the topography.
[18] W. Wulfhekel, U. Schlickum, and J. Kirschner, Microsc. Res. Tech. **66**, 105 (2005).
[19] U. Schlickum, N. Janke-Gilman, W. Wulfhekel, and J. Kirschner, Phys. Rev. Lett. **92**, 107203 (2004).
[20] A. Hubert and R. Schäfer, *Magnetic Domains: The Analysis of Magnetic Microstructures* (Springer, New York, 1998).
[21] T. K. Yamada, E. Martinez, A. Vega, R. Robles, D. Stoeffler, A. L. Vazquez de Parga, T. Mizoguchi, and H. van Kempen, Nanotechnology **18**, 235702 (2007).
[22] H. Zenia, S. Bouarab, J. Ferrer, and C. Demangeat, Surf. Sci. **564**, 12 (2004).